COBEM 2021 26th International Congress of Mechanical Engineering
November 22-26, 2021, Virtual Congress, Brazil

COB-2021-0830
A NUMERICAL STUDY OF BUOYANCY-INDUCED SMOKE FLOW IN REAL-SCALE EMERGENCY ENCLOSED STAIRS

Augusto Antoniolli Bolzoni
Ângela Gaio Graeff
Felipe Roman Centeno
Universidade Federal do Rio Grande do Sul (UFRGS), Rua Sarmento Leite, 425, Porto Alegre/RS
augustobolzoni@hotmail.com
angela.graeff@ufrgs.br
frcenteno@mecanica.ufrgs.br

Abstract. *Emergency enclosed stairs is one of the safety exit methods for evacuating people in a building during a fire. Brazilian standards define implementation parameters by analyzing the effective height of the building as well as its predominant occupation. The present work focuses on the analysis of an emergency enclosed stair in order to evaluate the buoyancy-induced smoke flow generated by different heat release rates of an ethanol pool fire placed at the ground floor of the building. The objective of this work is to evaluate the influence of buoyancy in the process of the smoke rising in the stairwell verifying the results of numerical simulations using the active or not activated stratification parameter. Based on these simulations, it is possible to see a flow of smoke along the stairwell due to the recirculation of hot gases between different stair landings, so it is analyzed related parameters such as velocity, temperature and pressure along the stairwell height, showing a decrease of the buoyancy driving force. For this study, numerical simulations are performed using the software Fire Dynamics Simulator (FDS), including a validation step based on an experimental work available in the literature for an 89.7 m high emergency enclosed stair, and then the analysis of the buoyancy driven smoke flow is conducted for the same geometry but changing the heat release rates of the fuel source, aiming to obtain numerical data for the parameters variation. The main conclusion is that velocity, temperature and pressure of the smoke flowing along the stairwell height are the most sensitive parameters in the buoyancy-induced phenomenon.*

Keywords: *FDS, Enclosed stairs, Stratification, Buoyancy, Smoke flow.*

1. INTRODUCTION

Nowadays in world, technological advances are extremely fast, always looking for an optimum design of processes in favor of the advancement of human race. With this advance there is a great concentration of people in small territorial spaces, leading to the so-called verticalization of buildings in large metropolises. The fact can be explained by Bejan (2016), being called the vascularization phenomenon, which is nothing more than the model of free evolution in the design of cities for the faster and more effective displacement of inhabitants or visitors. This comes from the constructal theory, to reduce loss of time in displacement from one destination to another, explaining the current scenario of larger buildings and agglomerates that include housing, work or mixed occupations, and in fact applies to countless people.

Agglomeration of people is one of the leading factors to increased imminent risk of fire, and in a tall building one way to have a safety scape in a fire occurrence is using a route by a protected stairwell. Then in the dedicated field of protection and prevention against fire there are resolutions and technical instructions made available at province level, for example, in the State of Rio Grande do Sul, there is the Technical Resolution No. 11 from Corpo de Bombeiros Militar do Rio Grande do Sul (2016). This technical resolution determines build and accessibility parameters of the stairwells. All these parameters are considered by the fire safety engineer to implement the required design to promote a safety scape from the building, without problems like smoke flood inside the stairwell, in example the implementation of a protected enclosed stair model.

In a more focused analysis, the data extracted from operational fire statistics of Corpo de Bombeiros Militar do Rio Grande do Sul (2021) – obviously disregarding missing data from small fires without the intervention of the institution – demonstrate that there is an increase in the indicators of fire situations over the last 4 years of analysis. With the open data from the year 2017 to 2021 it is possible to see in Figure 1 the increase of risk situations. With this increase risk of fire, a safe escape route in high-rise buildings with no smoke flood possibility should be extremely necessary.

There are several experimental studies about smoke flowing behavior inside stairwells. For example, Shi et al. (2014a) studied the effects of turbulent mixing and the stack effect of the hot smoke in high-rise buildings for 1/3-scale prototype building. They studied the variation of the velocity, mass loss rate of the fuel and temperature of the plume in the vertical direction along the stairwell.

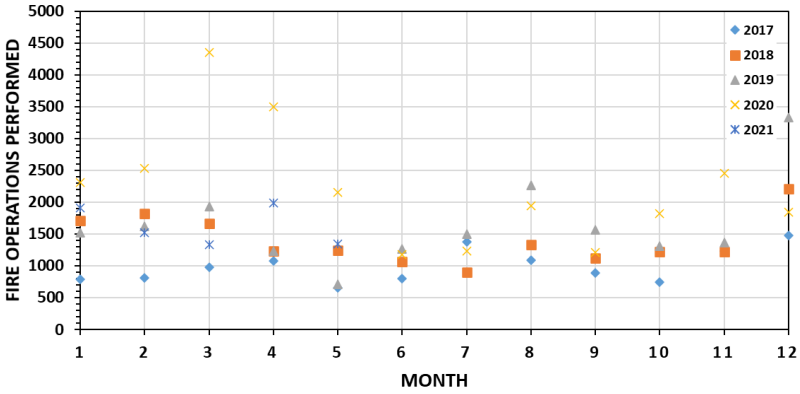

Figure 1. Fire operational statistics performed of the Corpo de Bombeiros Militar do Rio Grande do Sul from the year 2017 to 2021.

In another study, Shi et al. (2014b), using a 1/3-scale prototype building with fresh air entering at the bottom prototype, concluded that this air feed influences directly the heat release rate in the fire room positioned in a middle floor of the prototype. The purpose of that paper was to apply different opening sizes in the prototype windows. The variation in the entering air velocity has a direct influence in the buoyancy phenomenon occurred in the experiment.

An example of study that converges with Brazilian fire codes, is the study of the effectiveness in escape routes and access of fire fighters in high-rise residential buildings, where Hurley et al. (2016) determine the main application ideas for smoke control in stairs, being possible the application of elements of pressurization or application of crossed air flows by natural ventilation. As an auxiliary way to the air transport equations in these protection elements, Computational Fluid Dynamics (CFD) simulations are an auxiliary and commonly required tool due to the fact that the buildings have different construction features and layouts.

Ahn et al. (2020) performed a comparison of data obtained using a small-scale experimental bench and a computational simulation using Fire Dynamics Simulator (FDS), analyzing a 1/10-scale prototype building. In that article it is evaluated several parameters during the steady state period, such as smoke velocity, temperature, pressure and density. In that article, there is a comparation between experimental and numerical transient distribution of the rising smoke in the stairwell.

The purpose of the present paper is to perform numerical simulations of fires in enclosed stairs using the software Fire Dynamics Simulator (FDS), developed by the National Institute of Standards and Technology (NIST). Simulations are based on the experimental case previously studied in He et al. (2020), where smoke transport was analyzed in an 89.7m high stairwell. The present work consists on an analysis to validate the numerical simulation against experimental data for the real scale tests. After the validation of the software is demonstrated, a study is conducted by simulating 5 variations of Heat Release Rate (HRR) of the ethanol pool fire. It is also analyzed the flow of smoke on the levels of the protected staircase above the exit level of the smoke.

2. FIRE DYNAMICS SIMULATOR (FDS)

The software Fire Dynamics Simulator (FDS) is a free, public domain software developed by the National Institute of Standards and Technology (NIST) in partnership with the VTT Technical Research Center of Finland. It is a numerical simulation software based on CFD developed initially and mainly for fire modeling. It solves the fluid dynamic problem numerically by solving the Navier-Stokes-Equations adapted for low Mach numbers (Ma < 0.3) and using an explicit second-order predictor-correction scheme.

The software uses the Large Eddy Simulation (LES) methodology, although there is also the possibility of carrying out simulations through Direct Numerical Simulation (DNS). For the sub-grid turbulence modeling the software uses turbulence models based on the Boussinesq approximation of turbulent viscosity. In the present work, simulations are performed using the LES methodology and Deardorff turbulence model.

For domain discretization, FDS uses straight, uniform and staggered meshes. A staggered mesh is one that assigns scalar quantities to the center of the control volume, velocity components to the faces of the control volume, and vorticity components to the edges. The software also allows for the process of parallelization in the simulation which allows more than one computer processors, or more than one core in a single computer processor, to simulate a case with multiple meshes processed simultaneously, becoming a tool to reduce computational spent time.

The mathematical formulation that the FDS uses is represented in McGrattan et al. (2020). The continuity equation is listed in Eq.1, where ρ is the density, $\mathbf{u}$ the velocity components and $\dot{m}_b'''$ is the production rate of species α by evaporating droplets or particles. The transport equation of species is listed in Eq.2, where Z_α is the mass fraction of species α, D_α is the diffusivity of species α, $\dot{m}_\alpha'''$is the production rate of species α and $\dot{m}_{b,\alpha}'''$ is the production rate of

species α by evaporating droplets or particles. The momentum equation is listed in Eq.3, where $\boldsymbol{\omega}$ is the vorticity components, H is the stagnation energy per unit mass, $\tilde{p}$ is the perturbation pressure, $\mathbf{g}$ is the gravitational acceleration, $\mathbf{f}_\mathrm{b}$ the drag force exerted by the subgrid-scale particles and droplets, and τ is the viscous stress. The energy conservation equation is listed in Eq.4, where h_s is the sensible enthalpy, $\bar{p}$ is the background pressure decomposed from the resolved pressure, $\dot{q}'''$is the heat release rate per unit volume from a chemical reaction, $\dot{q}_b'''$ is the energy transferred to subgrid-scale droplets and particles, and $\dot{\mathbf{q}}''$ represents the conductive, diffusive and radiative heat fluxes.

$$\frac{\partial \rho}{\partial t} + \nabla.(\rho \mathbf{u}) = \dot{m}_b''', \tag{1}$$

$$\frac{\partial}{\partial t}(\rho Z_\alpha) + \nabla.(\rho Z_\alpha \mathbf{u}) = \nabla.(\rho D_\alpha \nabla Z_\alpha) + \dot{m}_\alpha''' + \dot{m}_{b,\alpha}''', \tag{2}$$

$$\frac{\partial \mathbf{u}}{\partial t} - \mathbf{u} \times \boldsymbol{\omega} + \nabla H - \tilde{p}\nabla\left(\frac{1}{\rho}\right) = \frac{1}{\rho}[(\rho - \rho_0)\mathbf{g} + \mathbf{f}_\mathrm{b} + \nabla.\tau], \tag{3}$$

$$\frac{\partial}{\partial t}(\rho h_s) + \nabla.(\rho h_s \mathbf{u}) = \frac{\mathrm{D}\bar{p}}{\mathrm{D}t} + \dot{q}''' + \dot{q}_b''' - \nabla.\dot{\mathbf{q}}'', \tag{4}$$

The stack effect is the buoyancy-induced air movement due to temperature differences between internal and external regions of a domain. In FDS, McGrattan et al. (2020) determines that for simulating this effect, it is necessary to include the entire building, or a fraction of it, both inside and outside, on the computational domain. This effect captures the pressure and density decrease in the atmosphere based on the temperature difference. The stratification term is correlated to the background pressure, being function of time and vertical spatial coordinate. By default, FDS assumes that the parameter stratification is active, but it can be deactivated, and in this way the software neglects the pressure and density decreases with height variation for routines.

3. PROBLEM STATEMENT

The validation process in this paper is above He et al. (2020) experimental problem. In that experimental problem, there were made tests to observe the smoke transport behavior with the variation of openings in a stairwell. The smoke tests were conducted on an 89.7m high stairwell. It was used an ethanol rectangular pool fire, and in the experiment, were measured the mass loss rate of the combustible, temperature in different highs on stairwell and the air velocity in the first-floor open door that feeds the combustion process. In that experiment, two doors were kept open during the combustion process, one in the first floor and the second in an upper floor – in the validation process, the fifth floor was adopted. All other openings were further sealed to reduce the air infiltration.

The validation of the numerical tool began with the division of the computational domain into 4 sub-regions. The first sub-region is the fire room, where the ethanol pool fire and the door through which fresh air enters the domain are located. The second sub-region is the internal domain of the staircase between the first floor and the fifth floor. The third sub-region is the exhaust gas room, where there is an outlet door for those resulting from combustion, such as particulates and combustion gases. The fourth sub-region is the fifth floor above, inside the stairs, where there are only concrete materials and the doors to the other floors, that are treated as closed with no leaks.

The computational domain can be seen in Figure 2, where in fact demonstrate the extension of the frontal domain (sub-region 1) at the entrance and exit doors by one hydraulic diameter, the position of the ethanol pool fire and some green dots which represents the position of the measuring devices. For each separate mesh, a computer processor – core – was applied in the MPI process.

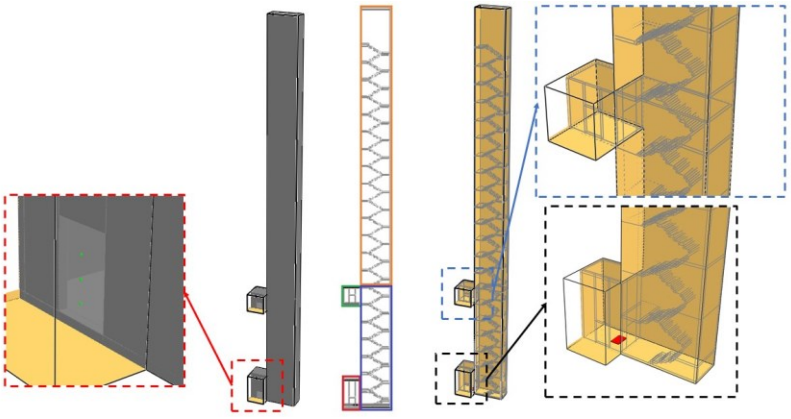

Figure 2. Whole domain of simulation.

3.1 Mesh resolution

The mesh resolution for the validation process was based on the method expressed by McGrattan et al. (2020), where the calculation of the characteristic fire diameter can be observed in Eq.5. Assuming that the correlation of the characteristic fire diameter (D^*) and the mesh resolution (δ) should be approximated from McGrattan (2007), it is expected that the correlation should be between 4 and 16. Taking into account the fact that the ambient temperature (T_∞) is 33 °C, the heat release rate ($\dot{Q}$) is about 860 kW, adopting other parameters for the smoke plume developing from Incropera et al. (2006) such as the ambient air density (ρ_∞) of 1.1614 kg/m³ at 300 K, ambient air specific heat (c_p) of 1.007 kJ/(kg·K) at 300 K. The mesh resolution adopted is 0.20 m, so the characteristic fire diameter obtained is 0.90, and the ratio (D^*/δ) = 4.50. The simulation starts with 254990 elements, and the spent computational time for validation was 40465.301s.

$$D^* = \left(\frac{\dot{Q}}{\rho_\infty c_p T_\infty \sqrt{g}}\right)^{\frac{2}{5}}, \tag{5}$$

3.2 Software validation

All information of the experimental tests of the stairwell was obtained from He et al. (2020), including geometric parameters, boundary conditions, fuel properties, measurements (types and positions). It must be emphasized that all 21 floors were implemented in the current numerical simulation, being this a highlight of the present work since previous published papers, in general, performed only simulations of small-scale stairwells or not high-rise stairwells, while here it is simulated a real-scale high-rise stairwell, with 89.7 m high.

Despite He et al. (2020) provides valuable data for that experiment, making it possible to simulate it numerically, some information is missing, such as the construction materials of the enclosed stair. Theoretically following Brazilian standards, Corpo de Bombeiros Militar do Rio Grande do Sul (2016) regulate the minimum fire resistance time of a wall in a protected region about 2 hours, being the experiment time a small fraction of all this time – a quarter-hour – so in Technical Instruction No. 8 of the Polícia Militar do Estado de São Paulo (2019), laboratory tests describe the concrete resisting for 1 hour and a half when it is 0.115 m thick. Thus, the numerical setup considered all walls made of concrete, 0.10 m thick.

In Table 1 it is possible to see values that were adopted for the validation step, in fact the environment conditions and heat of combustion were determined through He et al. (2020), the concrete thermal properties through Hurley et al. (2016) and a αt^2- ramp was applied to control the increase in combustion, where the value of α was selected as an ultra-fast-growing fire coefficient. Also, Table 1 express values of the burning process.

With this condition, Figure 3 shows that it takes about 68 s to reach the HRR of 860 kW, and analyzing the MLR, it is possible to see the behavior of the HRR respecting the αt^2-growth ramp between 0 and 68 s, and keeping the prescribed average value. The Heat Release Rate (HRR) of the ethanol combustion process was an input in the numerical software, obtained by Eq. 6, which is a function of the mass loss rate during the steady state period (MLR) and the combustion efficiency, being both values obtained from He et al. (2020).

Table 1. Values adopted for the validation.

Parameter	Value
Ambient temperature	33 ºC
Combustible	Ethanol
Mass of Combustible	24 kg
Heat of Combustion	26.8 kJ/g
Combustion Efficiency	0.92
Pool Fire Area	0.9744 m²
Burning Duration	792 s
Concrete Emissivity	0.94
Concrete Conductivity	1.40 W/(m.K)
Concrete Specific Heat	1.20 J/(kg.K)
Concrete Density	2500 kg/m³
α Coefficient	0.1876 kW/s²
Mass Loss Rate (MLR)	34.90 g/s
Heat Release Rate (HRR)	860 kW

$$HRR = MLR\varepsilon HC, \tag{6}$$

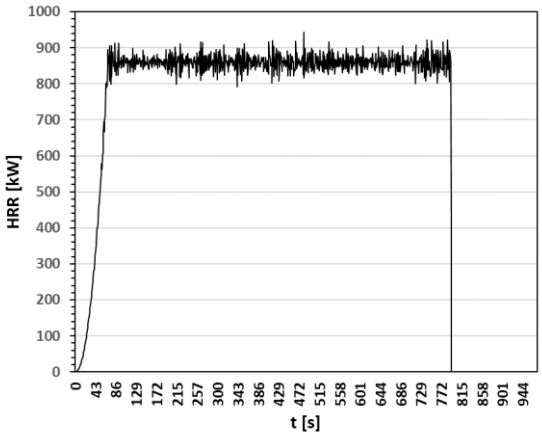

Figure 3. αt^2- ramp fire growth curve (ultrafast growth) and HRR analysis of the validation.

Using this methodology, the average mass loss rate found is 30.19 g/s, which is 13.47% smaller than the 34.9 g/s of the experimental test (this is a good agreement, but future works will look deeper at this methodology in order to get a better agreement for the MLR).

To obtain the required numerical measurements from the software, some numerical devices were implemented in a central column at the midpoint of the stairs, where in fact there is no concrete material, just an empty space that looks like a vertical shaft. These numerical devices were placed at the same positions as the measurement apparatus employed in the experiments of He et al. (2020). With these numerical devices, it is obtained temperatures calculated with the numerical software, to be later compared with the experimental data for temperatures. There are three more velocity devices at the front door on the ground floor, where fresh air feeds the combustion process.

For validation purposes, in addition to the MLR analysis presented above, it is possible to compare the temperature parameters in the vertical shaft and the velocity at the ground floor open door, making a comparison of the results obtained in the numerical simulation, and noting that in the experimental test, the authors reported that velocity and temperature measurements have measurement errors of less than 2%. To deal with the two extreme deviations, in Figure 4 it is possible to observe the largest error obtained from the thermocouple located at 5.60 m, between experiment and simulation and, it is also possible to observe the smallest one for the thermocouple located at 45.80 m.

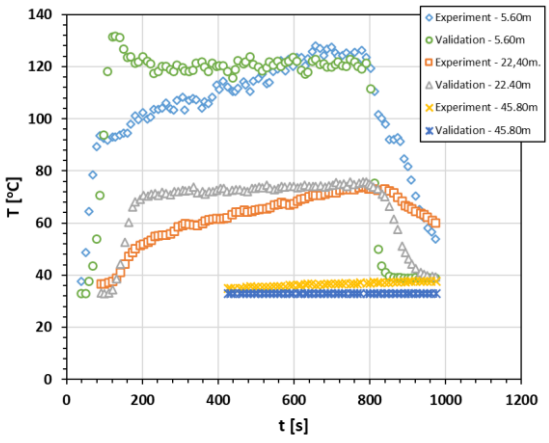

Figure 4. Difference obtained from thermocouple comportment between experiment and validation.

Numerical devices positioned on the central axis of the stairs promote some divergences from the experimental test, In Table 2 it is possible to see the results of the average error of the temperature measurement. The average error analyzed for each sensor follows as discussed in Eq. 7.

$$\overline{Error} = \overline{\sum_{t=0}^{t=975} \left| \frac{T_{experiment,(t)} - T_{simulation,(t)}}{T_{experiment,(t)}} \right|}, \tag{7}$$

Table 2. Average temperature measurement validation error.

Sensor height position	Average error
Thermocouple at 5.60m	18.56%
Thermocouple at 10.10m	17.57%
Thermocouple at 14.60m	13.96%
Thermocouple at 15.80m	12.65%
Thermocouple at 22.40m	15.86%
Thermocouple at 26.30m	14.16%
Thermocouple at 30.20m	14.18%
Thermocouple at 34.10m	17.19%
Thermocouple at 38.00m	16.17%
Thermocouple at 41.90m	11.78%
Thermocouple at 45.80m	9.39%

It is important to highlight that, although the graphical results seem to be biased, the strongest parameter to be observed is the average MLR, which is the guide for the combustion of the ethanol pool fire. The last parameter that must be analyzed is the velocity at the open front door, where fresh air feeds the ethanol combustion on the first floor. The average velocity at the 3 heights at which the sensor was adopted – 0.5m, 1.0m and 1.5m – should be 1.76 m/s from the experiment article, while the simulation results showed that the average velocity between the three sensors is 1.55 m/s, thus a deviation of only 12.19%.

4. RESULTS AND DISCUSSIONS

A total of ten numerical simulations were run in the software FDS in order to numerically analyze the effect of the buoyancy-induced smoke flow in the emergency enclosed stair. For all these 10 simulations, all input parameters as domain discretization (mesh), geometric characteristics of the stairs and amount of fuel in the ethanol pool fire were kept as in He et al. (2020). The only difference from the validation presented previously being the adoption of 5 different values of HRR (Heat Release Rate), which are listed in Table 3, and with these values fixed, two simulations were carried out for each value of HRR, one simulation with the stratification condition activated – the FDS's default condition – and a simulation with the stratification disabled. In this manner, besides the effect of different HRRs, which means different energy inputs into the domain, it was possible to analyze the effect of the stratification, which takes into account the variation of ambient pressure and density as a function of the vertical coordinate (along the building height).

Table 3. Simulation cases studied.

HHR	Average MLR	Burn duration	αt^2 RAMP duration	Computing time
286kW – Stratification ON	10.532g/s	2274s	40s	74764.4 s
286kW – Stratification OFF				66365.6 s
573kW – Stratification ON	20.665g/s	1158s	56s	49210.9 s
573kW – Stratification OFF				44139.1 s
860kW – Stratification ON	30.198g/s	792s	68s	40465.3 s
860kW – Stratification OFF				36070.6 s
1146kW – Stratification ON	39.062g/s	612s	79s	32753.3 s
1146kW – Stratification OFF				35116.3 s
1433kW – Stratification ON	47.212g/s	506s	88s	24937.1 s
1433kW – Stratification OFF				15752.8 s

Figure 5, Figure 6 and Figure 7 shows the data obtained from thermocouples (temperature sensors, Figures 5(a) and 5(b)), velocity sensors (Figures 6(a) and 6(n)) and pressure sensors (Figures 7(a) and 7(b)) located in the vertical shaft of the stair. The data are shown for numerical measurements positioned only at two heights, being a region close to the fire room (5.60 m high) and a region close to the exit room at the fifth floor (22.40 m high). It is possible to see a variation in the maximum and average values when different values of HRR are considered, and a behavior of the phenomenon induced by buoyancy can also be seen. Between active and non-active stratification, there is a smooth variation in the analysis of the same HRR, which is expected because the entire enclosed stair domain was implemented in the FDS software, and according to McGrattan et al (2020), stratification shows results efficiently varied when only a part of the domain is entered in the software so that the variation of pressure, density and temperature does not have the whole domain to develop the flow. However, it is relevant to analyze the temperature increase directly proportional to the HRR increase, as well as the smoke velocity and the internal pressure of the enclosed stair. This means that increasing the HRR,

more energy is available to both increase the smoke temperature, as expected, and also to push the smoke upwards, as can be seen by the increase in the velocity.

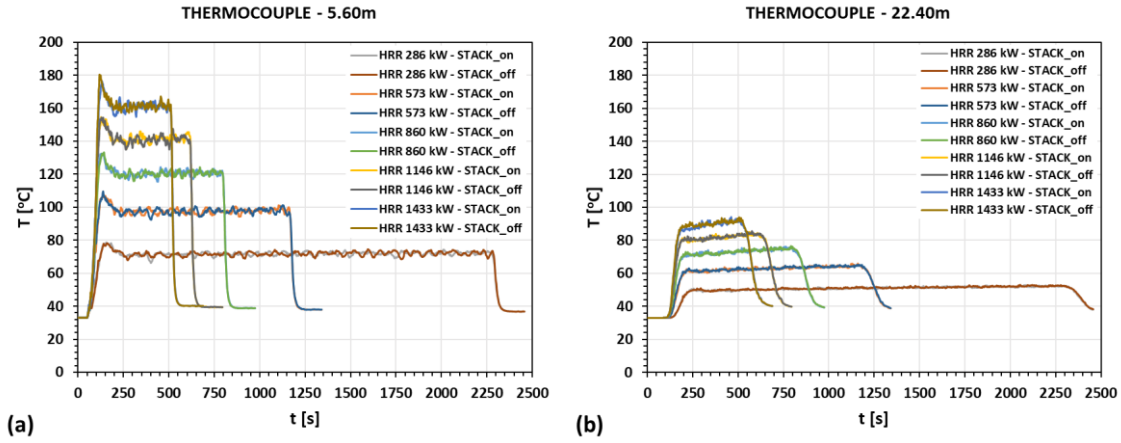

Figure 5. Numerical results obtained for temperatures (a, b).

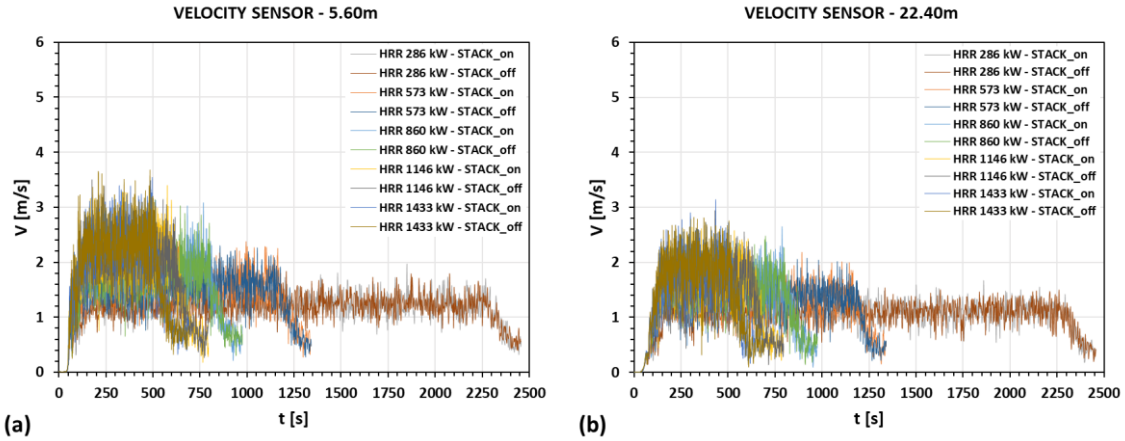

Figure 6. Numerical results obtained for velocity (a, b).

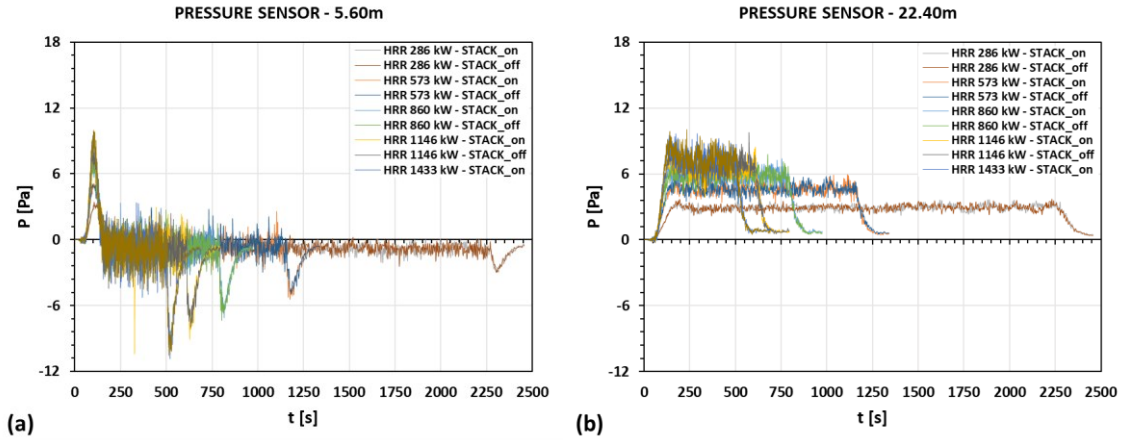

Figure 7. Numerical results obtained for pressure (a, b).

Different from the analysis of variation of temperature, velocity and pressure over time as presented, analyzing the mean values of temperature, velocity and pressure in the steady state of the combustion process, varying with height, it is possible to verify in Figure 8 the actual influence of stratification, where the curves of the comparison do have a similar behavior. It is interesting to note in Figure 8 that the temperature has its peak close to the ground, since the pool fire is

placed there, and decreases smoothly up to about 22 m high, since the fifth floor is open (exit room). Above the fifth floor, the smoke temperature drop increases until it reaches the ambient temperature at a height of approximately 40 m, and above that it remains steady at ambient temperature (33 °C). Also shown in Figure 8, the smoke velocity first increases close to the ground floor, since the smoke first flows through the door that connects the fire room and the stairwell, being accelerated due to the suction effect. As the smoke flows upwards, its temperature decreases and then its velocity also decreases, since this is basically a buoyancy-driven flow, pushed by temperature gradients. As the smoke reaches the fifth floor (22.4 m high), its velocity is slightly increased since it reaches the open door of the exit room. Velocity decreases again as the temperature decreases, until reaching the ambient temperature at 40 m, where the smoke velocity is zero. Finally, Figure 8 shows pressure profiles along the vertical axis of the stairwell, showing that pressure is continuously increased with height since the temperature is decreased, then smoke becomes denser, until 40 m where the temperature becomes constant as well as smoke density and pressure. As HRR is increased, temperature, velocity and pressure are increased but follow the same behavior over the stairwell height as described. It is also noteworthy that the behavior described above is the same independently of the fire power (HRR), i.e., temperature, velocity and pressure reach a constant value at 40 m high and above, while one could expect that smoke keeps flowing to higher levels as HRR is increased, which is not seen in Figure 8. Regarding the effect of stratification, it is not noticed an important influence of it on any of the parameters and positions shown in Figure 8 - this result is unexpected and worth further investigation in the future, since the building is 89.7 m high and so stratification would be noticeable due to ambient pressure gradients outside the building.

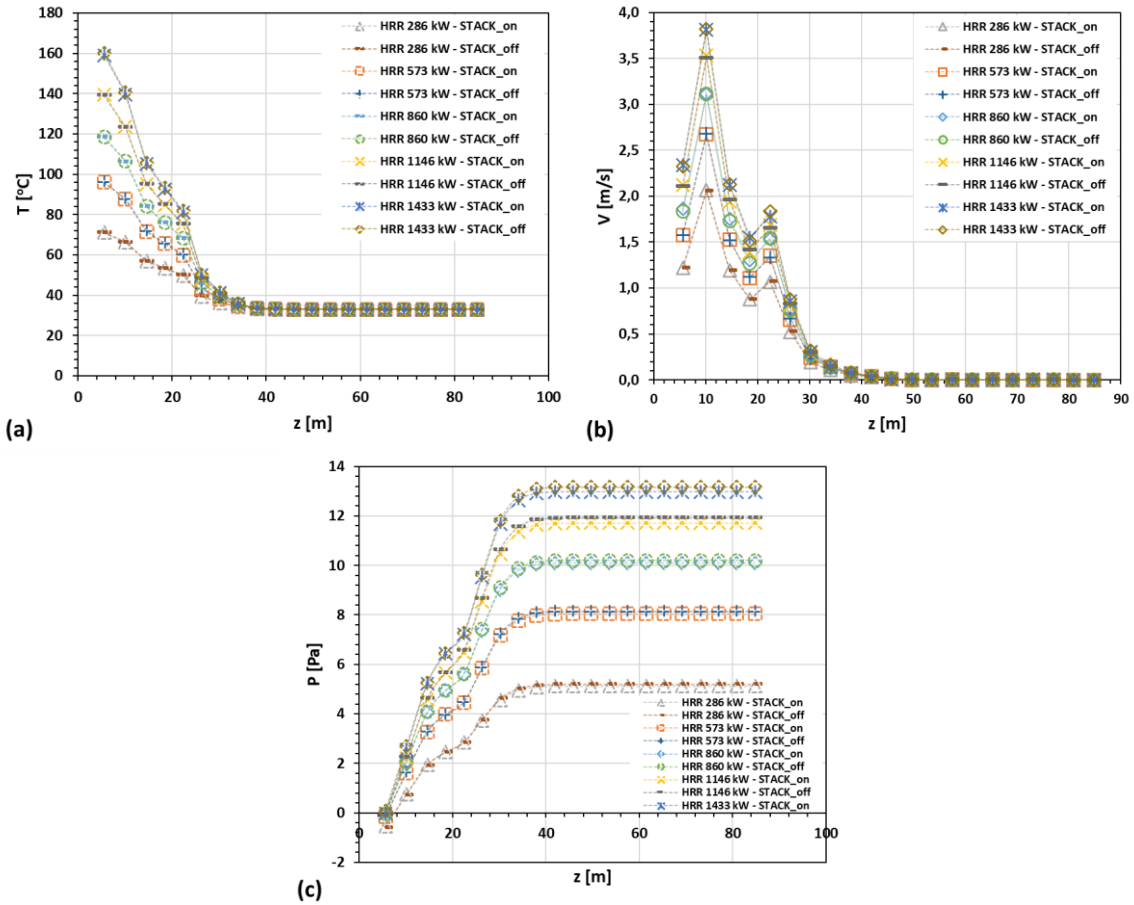

Figure 8. Variation over height of mean values of temperature (a), velocity (b) and pressure (c) during the steady state period.

Figure 9 shows averaged values (during steady state) of temperature and velocity along the z axis of the stairwell for various fire powers (HRRs). In this figure, z is scaled by $Q^{2/5}$ and V is scaled by $Q^{1/5}$ (here Q refers to the HRR), being these scaling taken from McCaffrey (1979), which studied the classical plume under open-air conditions.

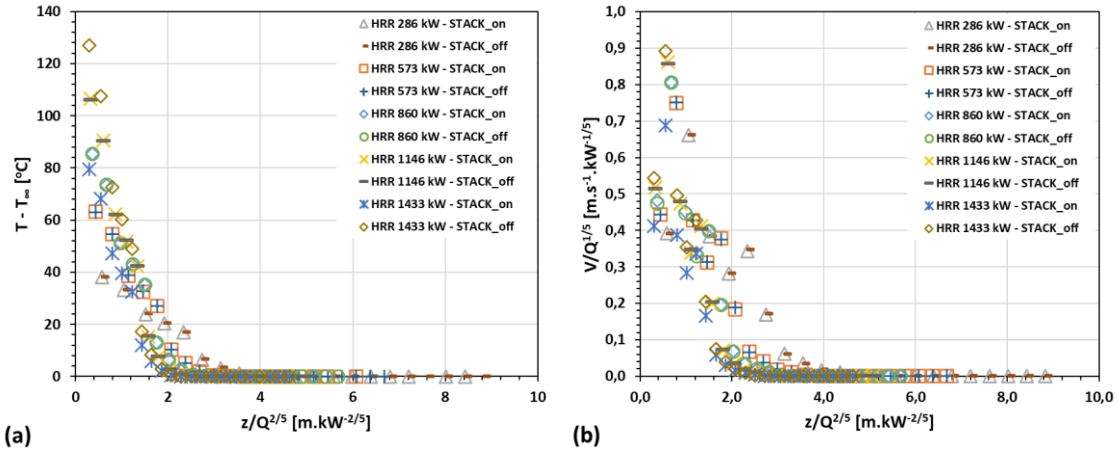

Figure 9. Temperature (a) and velocity (b) (averaged during steady state) distributions along the z axis of the stairwell for various fire powers. (z is scaled by $Q^{2/5}$ and V is scaled by $Q^{1/5}$).

Figure 9 shows that temperature and velocity curves are reasonably collapsed into one curve (for each parameter, T and V) when the scaling is introduced, despite some scattering of the numerical data is still present; such scaling was introduced by McCaffrey (1979) for plumes under open-air and then in that work both temperature and velocity curves are collapsed into one curve for each parameter, while the present study deals with a plume in a closed environment (the stairwell), even though there is some scattering in Figure 9, it is considered that such scaling is at least reasonable for this scenario. A similar behavior (with some scattering) was found by Ahn et al. (2020) when applying McCaffrey's scaling to another stairwell.

Figure 10 presents smoke rising times for various fire powers (HRRs), where the horizontal axis of Figure 10(a) is the smoke height (z) at a given time (s) and the horizontal axis of Figure 10(b) is the scaled smoke height ($z^{4/3}/Q^{1/3}$), being this scaling taken from Ahn et al. (2020). It is observed in these figures that the smoke needs more time to reach a given height as the HRR is decreased, which is in close agreement with velocity results presented in Figure 8 (i.e., smaller HRR leads to lower smoke velocities). It is also observed that the scaling employed for the smoke rising time was not adequate for the present study, since Figure 10(b) data is more scattered than data in Figure 10(a), while the first is not scaled by $z^{4/3}/Q^{1/3}$. As an illustration of the smoke displacement, Figure 11 depicts snapshots of temperature fields during smoke ascent for a variety of heights and times, spanning from a time of 50.72 s when the smoke reaches 5.60 m, to a time of 676.67 s when the smoke reaches 41.90 m.

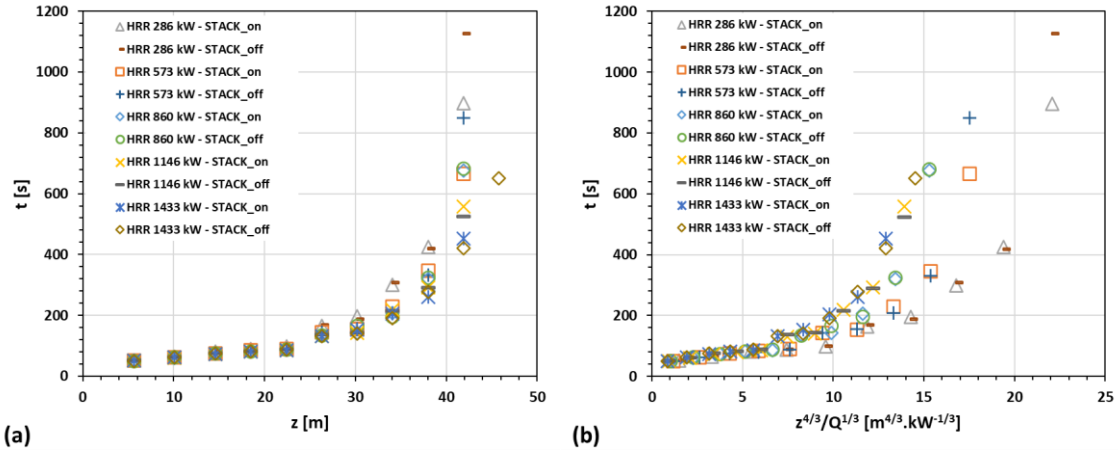

Figure 10. Smoke rising time for various fire powers: (a) horizontal axis is the smoke height (z) and (b) horizontal axis is the scaled smoke height ($z^{4/3}/Q^{1/3}$).

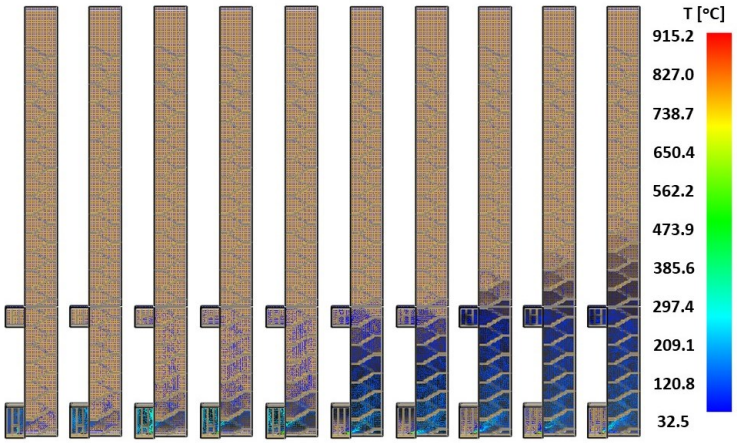

Figure 11. Temperature snapshots during smoke ascent. Images from left to right: smoke reached 5.60 m at 50.72 s, 10.10 m at 60.47 s, 14.60 m at 74.12 s, 18.50 m at 80.94 s, 22.40 m at 86.79 s, 26.30 m at 136.51 s, 30.20 m at 142.36 s, 34.10 m at 206.72 s, 38.00 m at 319.82 s and 41.90 m at 676.67 s.

5. CONCLUSION

This paper numerically studied the buoyancy-driven smoke flow in a real-scale, 89.7 m high, enclosed stair of a high-rise building using the software FDS. Validation of the numerical tool was performed based on an experimental work of a similar case, comparing results of FDS to the measurements and obtaining a good agreement between them. The mesh employed in these simulations was verified by analyzing the ratio of the characteristic fire size and the grid size, for which there is a recommended range reported in the literature and the employed mesh fits within to that range.

Regarding the analysis of the buoyancy-induced phenomenon, it is noticeable that the higher the HRR applied in the simulations, the faster the ascent of smoke from the first floor to the fifth floor. This is fateful analyzing the graphs of temperature, velocity and pressure variation over time, that is, the greater heat supplied, faster the advance speed as the height varies, as well as the temperature reaches higher levels and the pressure turns out to be high due to the fact that the rest of the stairwell is treated as a hermetically sealed case. Above 45.80 m there were practically no variations in the sensor's readings, due to the fact that the fifth-floor door is open and makes the gas exit velocity have greater relevance compared to the thermal potential of the buoyancy-induced phenomenon.

Applying a scalar on the horizontal axis to correlate velocity and temperature, it is able to certify that in fact the behavior of the effects is similar. Finally, it is evident that the time to reach a certain time with height variation becomes longer when there is a low HRR value, so there is a longer period for the sensors to be able to read the pressure, velocity and temperature variations, explaining by the buoyancy-induced phenomenon.

Concluding the analysis of this work, the buoyancy effect is finally explained by the variation of the temperature, velocity and pressure conditions of the convective plume of the combustion gases, being directly linked to the combustion power. Merely the stratification parameter correlation values on or off in the software have no real interference for small HRRs values, where the buoyancy is not as solicitous compared to larger HRRs. With this, it is only once more evident that the buoyancy-induced phenomenon in natural ventilations is due to the pressure and temperature that will generate the thermal potential differential to promote the internal flow in the enclosed stair.

6. REFERENCES

Ahn, C., Kim, D., Park, C., Kim, M., Kim, T., Bang, B., An, S., Yarin, A. L., Yoon, S. S. (2020) "Experimental and numerical study of smoke behavior in high-rise stairwells with open and closed windows." *International Journal of Thermal Sciences*, Vol. 157, p. 106500. http://dx.doi.org/10.1016/j.ijthermalsci.2020.106500.

Bejan, A. (2016). "The Physics of Life: the evolution of everything". New York: St. Martin'S Press. 272 p.

Corpo de Bombeiros Militar do Rio Grande do Sul. (2016) Divisão Técnica de Prevenção de Incêndio e Investigação. RESOLUÇÃO TÉCNICA CBMRS Nº 11 – PARTE 01: SAÍDAS DE EMERGÊNCIA. Disponível em: https://www.bombeiros-admin.rs.gov.br/upload/arquivos/201706/01155612-rtcbmrs-n-11-parte-01-2016-saidas-de-emergencia-versao-corrigida.pdf. Acesso em: 07 jun. 2021.

Corpo de Bombeiros Militar do Rio Grande do Sul. (2021) Estatísticas Operacionais. Disponível em: https://www.bombeiros.rs.gov.br/estatisticas-operacionais. Acesso em: 07 jun. 2021.

He, J., Huang, X., Ning, X., Zhou, T., Wang, J., Yuen, R. (2020) "Stairwell smoke transport in a full-scale high-rise building: influence of opening location". *Fire Safety Journal*, Vol. 117, pp. 103151. http://dx.doi.org/10.1016/j.firesaf.2020.103151.

Hurley, M.J., Gottuk, D.T., Hall Jr., J.R., Harada, K., Kuligowski, E.D., Puchovsky, M., Torero, J.L., Watts Jr., J.M., Wieczorek, C.J. (2016). "SFPE Handbook of Fire Protection Engineering". Springer-Verlag New York. *Society of Fire Protection Engineers*. 3493. doi: 10.1007/978-1-4939-2565-0

Incropera, F. P., DeWitt, D. P., Bergman, T. L., & Lavine, A. S. (2006). Fundamentals of heat and mass transfer (6th ed.). Nashville, TN: John Wiley & Sons.

McCaffrey, B. (1979) "Purely buoyant diffusion flames: some experimental results", Final Report, Chemical and Physical Processes in Combustion, The National Institute of Standards and Technology (NIST), Miami Beach, p. 49.

McGrattan, K. (2007) Verification and Validation of Selected Fire Models for Nuclear Power Plant Applications – Volume 7: Fire Dynamics Simulator (FDS), NUREG-1824, United States Nuclear Regulatory Commission and Electric Power Research Institute.

McGrattan, K., Hostikka, S., Floyd J., McDermott, R., Vanella, M. (2020). "Fire Dynamics Simulator, Technical Reference Guide Volume 1: Mathematical Model". *National Institute of Standards and Technology*, Gaithersburg, Maryland, USA. http://dx.doi.org/10.6028/NIST.SP.1018

Polícia Militar do Estado de São Paulo. (2019) INSTRUÇÃO TÉCNICA Nº 08/2019: SEGURANÇA ESTRUTURAL CONTRA INCÊNDIO. Disponível em: https://www.bombeiros-admin.rs.gov.br/upload/arquivos/201908/02113750-it-08-2019.pdf. Acesso em: 08 jun. 2021.

Shi, W.X., Ji, J., Sun, J.H.; Lo, S.M., Li, L.J., Yuan, X.Y. (2014a) "Influence of fire power and window position on smoke movement mechanisms and temperature distribution in an emergency staircase." *Energy And Buildings*, Vol. 79, p. 132-142. http://dx.doi.org/10.1016/j.enbuild.2014.02.083.

Shi, W.X., Ji, J., Sun, J.H., Lo, S.M., Li, L.J., Yuan, X.Y. (2014b) "Influence of staircase ventilation state on the airflow and heat transfer of the heated room on the middle floor of high rise building." *Applied Energy*, Vol. 119, p. 173-180. http://dx.doi.org/10.1016/j.apenergy.2013.12.055.

7. RESPONSIBILITY NOTICE

The author(s) is (are) the only responsible for the printed material included in this paper.